EES Solar

PAPER

View Article Online
View Journal | View Issue

Cite this: *EES Sol.*, 2025, **1**, 1040

Self-adaptive interfacial cooling for sustainable energy–water cogeneration in photovoltaics

Yang Zhao,[a] Kaitao Chen,[a] Feng Wang,[a] Chao Cheng,[b] Dan Gao,[abc] Heng Zhang,*[ad] Jiang Yan[e] and Yuting Wang[f]

The simultaneous production of electricity and freshwater *via* solar energy offers a promising approach to addressing global energy and water challenges. Here, we present a self-adaptive interfacial evaporation-driven photovoltaic energy–water cogeneration (IEWC) system that passively integrates thermal regulation with atmospheric water harvesting to enhance photovoltaic (PV) performance. By coupling a commercial PV module with a hydrophilic thin-film evaporator, the system enables efficient heat extraction and adaptive evaporative cooling, reducing surface temperature and suppressing thermal losses. Outdoor testing demonstrated a power output increase of 8.4% and a temperature reduction of up to 23 °C compared to standalone PV modules. Life-cycle techno-economic analysis shows that IEWC consistently yields the lowest relative operational level (ROL) among various PV cooling strategies across discount rate scenarios. Under a 5% technological improvement assumption, projected annual savings reach USD 17.48 billion (1.6‰ of global GDP), alongside notable reductions in CO_2 emissions, land use, and freshwater demand. The system performs reliably under variable outdoor conditions, making it suitable for off-grid and arid deployments. These findings highlight IEWC as a scalable, energy-autonomous solution for integrated power and water generation, with strong potential to advance sustainable and resilient solar infrastructure.

Received 17th September 2025
Accepted 19th September 2025

DOI: 10.1039/d5el00150a

rsc.li/EESSolar

Broader context

Photovoltaics (PV) are essential to global decarbonization, but high operating temperatures reduce efficiency and waste valuable thermal energy. Conventional cooling solutions often overlook heat recovery and add complexity or cost, limiting system sustainability. Here, we introduce a self-adaptive interfacial evaporative cooling (IEWC) strategy that passively regulates PV temperature and recovers low-grade thermal energy using ambient water and solar input alone. Our integrated approach enhances overall solar energy utilization without requiring active components or external energy sources. Experiments show that IEWC improves electricity generation by 8% while enabling simultaneous thermal energy recovery. Life-cycle and techno-economic analyses further demonstrate that IEWC reduces operational costs and broadens the economic viability of PV systems under diverse conditions. This dual-generation concept supports high-efficiency, low-cost solar deployment in arid, off-grid, or resource-constrained settings. By integrating power and heat production, the system advances the energy–water nexus and promotes circular resource use. Our results highlight a scalable, multifunctional pathway to maximize solar energy output, contributing directly to global goals for affordable clean energy and climate resilience.

1 Introduction

Freshwater and electricity are foundational to modern civilization and its sustainable development.[1,2] As the global population grows and climate change accelerates, the demand for sustainable and clean resources has reached a critical point.[3] There are many inefficiencies, environmental pollutants, and costs associated with conventional energy and water generation systems.[4–6] Solar energy is plentiful, renewable, and eco-friendly; the dual capability of solar energy to produce electricity and clean water has drawn considerable interest for its potential to address the global energy–water nexus crisis.[7]

However, photovoltaic (PV) panels that are directly heated by sunlight will convert only a fraction of the incident solar energy to electricity, with the rest lost to excess heat.[8–10] This excess heat can lead to considerable temperature increases, which therefore decreases the power conversion efficiency (PCE) and reduces the life of the system.[11,12] For example, for every 10 °C that the temperature increases, PCE falls approximately 5%, while the aging rate of the panels will be doubled. Therefore,

[a]*School of Energy, Power and Mechanical Engineering, North China Electric Power University, Beijing, 102206, China. E-mail: zhangchongheng@ncepu.edu.cn*
[b]*National Institute of Energy Development Strategy, North China Electric Power University, Beijing, 102206, China*
[c]*State Key Laboratory of Alternate Electrical Power System with Renewable Energy Sources, North China Electric Power University, Beijing, 102206, China*
[d]*Beijing Key Laboratory of Pollutant Monitoring and Control in Thermoelectric Production Process, North China Electric Power University, Beijing, 102206, China*
[e]*School of Electronic Science and Engineering, National Laboratory of Solid-State Microstructures, Nanjing University, Nanjing, 210023, China*
[f]*Institute of Thermal Energy Engineering, School of Mechanical Engineering, Shanghai Jiao Tong University, Shanghai, 200240, China*

appropriate thermal management is critically important if PV systems are to last long term and/or if their service efficiency is to be maintained.[8,13]

Working around this issue, researchers have devised solar-driven water–electricity cogeneration systems that can effectively harvest solar energy to generate both freshwater and PV electricity.[14–17] Broadly speaking, we can categorize these systems into two groups: (1) evaporation induced electricity generation and (2) heat-flow based power–water cogeneration.[15,18–21] The first approach utilizes electrochemical or osmotic gradients that can be obtained from the evaporation of water; however, this process tends to be unstable and has limited scalability.[22,23] The second approach typically combines PV modules with solar steam generators or thermoelectric generators (TEGs), and enables once-through thermal energy recycling.[24,25] Despite the presence of fouling from salt, inefficient energy conversion, and thermal mismanagement across subsystems,[23,26] both active and passive cooling technologies for PV systems exist.[27,28] Active cooling typically includes the use of forced fluid (*e.g.*, air and water) circulation with the need for external energy to operate forced fluid systems; thus, actively cooled PV systems require energy to operate and are systemically more complex.[29–32] Passively cooled PV systems, including systems that perform cooling *via* the spontaneous processes of radiative cooling, phase change materials (PCMs), and evaporative cooling, are less expensive and do not require additional energy, as these systems are purely passive.[5,33–35] Some passive cooling technologies have shown promise toward lowering PV cell temperature and improving system efficiency[35,36] but are still subject to trade-offs for water loss compared to cooling effectiveness or introducing unique complexities to the design.[37] Recent advancements in both passive systems and active cooling introduce great possibilities for improving the performance of a PV system.[28] For example, systems such as radiative cooling, PCMs, and evaporative cooling show potential to increase operational efficiency based on multiple prior studies.[5,11] Moreover, the passive cooling systems mentioned above are relatively inexpensive (at least compared to active systems) because they are passive processes and do not need a power source external to the system.[38] The passive methods noted above evade even greater complexity of design optics and maintain water loss/cooling effectiveness trade-offs.[39] Most importantly, existing solar cogeneration platforms are not regulated to a self-regulating system, thus limiting long-term performance and suitability under variable environmental conditions.[40]

In response to these obstacles and to encourage operational synergies between energy subsystem and water subsystem together, we offer a modular climate-adaptive Interfacial Evaporation-driven Photovoltaic Energy–Water Cogeneration (IEWC) system comprising three major components: a commercially available PV module, a thin-film hydrophilic wicking evaporator, and an active water management unit. The evaporator is thermally bonded directly to the back of the PV module by a thermally conductive interface and relies on passive capillary-action dripping of water through the evaporator, thereby producing interfacial evaporation of the water and continuous evaporation and conduction of heat away from the PV module, and inherent cooling of the PV cells.

The IEWC system is designed with a microcontroller which introduces adaptive control strategies to manage thermal effectiveness and inherent water efficiency despite dynamic environmental conditions. The IEWC system incorporates multiple sensors that detect real time parameters of solar irradiance and water levels, and the system manages pump use efficiently and implies that it only turns pumps on/off based on its own thermal management performance as an autonomous system of overall optimal water and latent heat use. The integrated nature of the IEWC system allows for a synergistic use of solar energy: solar energy converted to electricity, and unconverted solar energy into latent heat-driven evaporation. The IEWC system implements closed-loop siphon circulation which resolved water wasting as part of its operation.

The proposed IEWC system represents resilient, modular, operational, economically viable and scalable demonstration of sustainable energy–water cogeneration, particularly relevant to disconnected or arid regions, and resource constrained areas of the world. It has a passive thermal design, and real time adaptive control with a unique modular approach that, as presented, supports long term durability and economic value. This work demonstrates a new means of developing the field centered around synergistic evasion of interfacial evaporation and intelligent, real-time control, to materially improve both the freshwater produced and the power conversion efficiency of both co-generation products in an iterative integrated system.

2 Results and discussion

2.1. IEWC system design

The Interfacial Evaporation-driven Photovoltaic Energy–Water Cogeneration (IEWC) system features a modular and scalable architecture that enables simultaneous electricity generation, evaporative cooling, and freshwater production within a compact form factor. As illustrated in Fig. 1a, the system consists of three core components: a photovoltaic (PV) module, a hydrophilic thin-film evaporative cooling layer, and a water management unit. These subsystems are vertically integrated to facilitate efficient thermal and mass exchange. The system's operational modes under different conditions are shown in Fig. 1d–f.

The evaporative cooling layer, used in this study, is a commercial nonwoven hydrophilic fabric (polyvinyl alcohol-based, 3M, thickness $\approx$1 mm), which enables efficient capillary-driven water transport and uniform evaporation. This layer is thermally coupled to the backside of the PV module *via* a commercial conductive silicone pad (3M, thermal conductivity $\approx$ 2.5 W m^{-1} K^{-1}, applied thickness $\approx$0.3 mm), serving as the thermal interface material (TIM) to ensure efficient transfer of residual heat from the solar cell to the evaporator. This hydrophilic layer passively draws water from the underlying reservoir through capillary action and facilitates continuous interfacial evaporation, which removes latent heat, lowers the PV operating temperature, and contributes to water vapor generation. A capillary siphon mechanism maintains a closed-

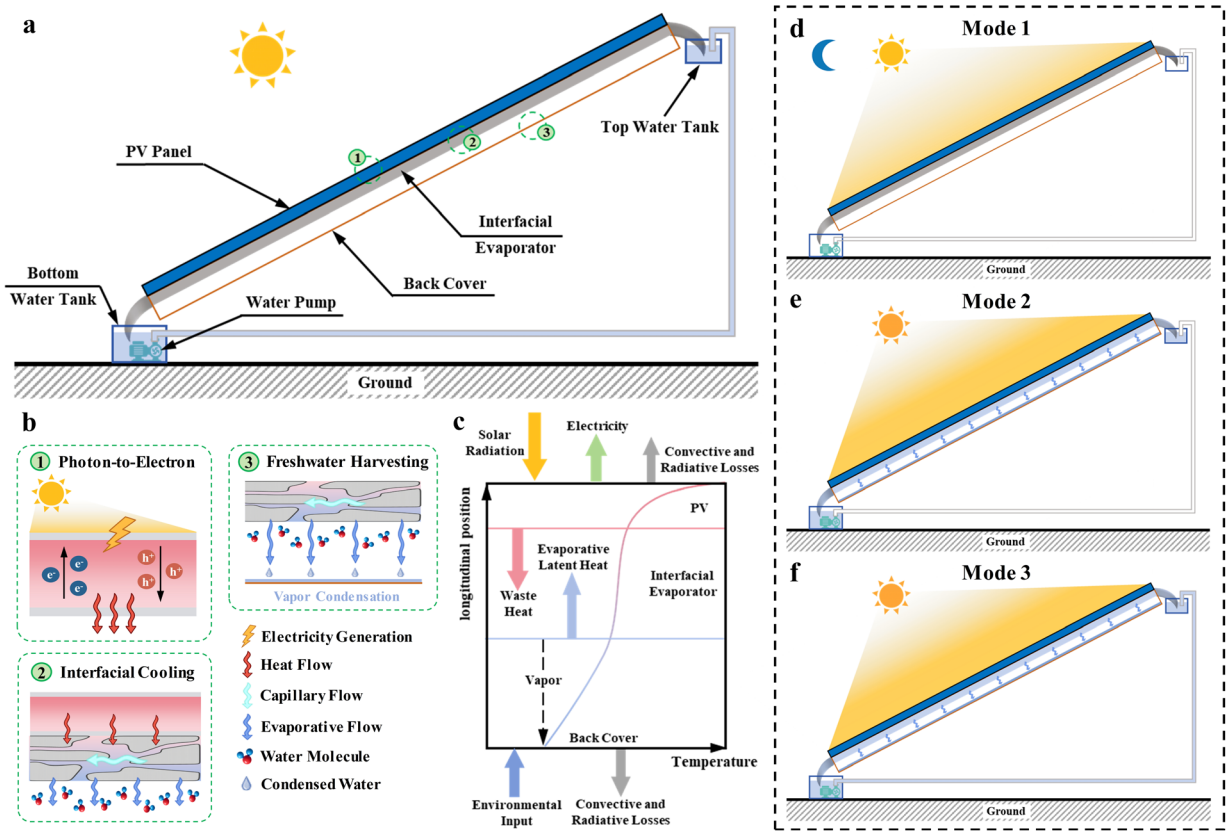

Fig. 1 Design of the IEWC system. (a) Schematic illustration of the IEWC system comprising a photovoltaic (PV) module, a hydrophilic wicking evaporative cooling layer, and a water management unit. The evaporative layer is attached to the rear side of the PV panel to dissipate heat through interfacial evaporation, while a capillary siphon mechanism enables a closed-loop water circulation, synergistically enhancing energy and water utilization. (b) Schematic of the coupled thermodynamic and hydrological processes: (1) solar absorption and electricity generation; (2) interfacial evaporation cooling; (3) vapor condensation. The capillary siphon enables continuous water replenishment. (c) Diagram of the energy and mass transfer pathways within the IEWC system. Yellow arrow indicates solar energy input; green arrow indicates photovoltaic electricity generation; red arrow indicates heat dissipation to the evaporator; light blue arrow represents latent heat removal *via* evaporation; gray arrows denote convective and radiative losses to the ambient air; blue arrow represents the environmental input; and dashed arrows show the flow path of water within the system. (d–f) Schematic representations of three operating modes of the IEWC system under different conditions: (d) Mode 1, the system during the night, with minimal solar energy input; (e) Mode 2, the system with water in the upper tank under high irradiance and at high PV panel temperature; (f) Mode 3, the system with pump operation triggered by insufficient water level in the upper tank under high irradiance and at high PV panel temperature, optimizing energy and water utilization.

loop water supply without external energy input, enabling pump-free autonomous cooling. A small auxiliary pump is included in the design only to replenish the upper tank when the water level drops below a threshold, but this does not affect the cooling function, which is entirely realized by passive interfacial evaporation (see Fig. 1f). Due to the high humidity inside the closed system and the cooler surface on the backside of the PV panel, condensation naturally occurs at the surface near ambient temperature. This process is also passive and does not require external energy input. The collected condensate can be recirculated back into the system, though this feature has not yet been experimentally validated in this study. Future work will explore the integration of thermoelectric generation using the temperature gradient created by the condensation process (TEG or moisture sorbent based direct energy generation[41,42]). This addition will enhance the overall efficiency of the system by enabling energy harvesting from temperature differences, further improving its sustainability and applicability in remote or off-grid regions.

The integrated operation of the IEWC system involves a coupled thermodynamic and hydrological process comprising three main stages. First, solar radiation is absorbed by the PV module, where a portion is converted into electricity, while excess thermal energy is transferred to the evaporative cooling layer *via* a thermally conductive interface. Second, water drawn from the reservoir through capillary action undergoes interfacial evaporation, extracting latent heat from the system. This passive cooling lowers the PV temperature, enhances power conversion efficiency, and simultaneously generates water vapor. Third, the generated vapor is subsequently condensed into freshwater within the closed-loop system, ensuring simultaneous cooling and water recovery. These coupled processes are schematically illustrated in Fig. 1b, highlighting the fully passive and self-sustained nature of the system.

The energy and mass transfer pathways are further summarized in Fig. 1c, where solar radiation acts as the primary input, and latent heat removal, convective and radiative losses, and internal water recycling are effectively coordinated to maximize system efficiency. This passively driven, integrated design offers a practical and scalable solution for energy–water cogeneration in remote or arid regions.

2.2. IEWC working mechanism

Building upon the structural integration detailed in Section 2.1, this section focuses on the underlying thermodynamic and mass transport mechanisms that enable the IEWC system to realize simultaneous photovoltaic cooling, water evaporation, and energy conversion. The central physical process—interfacial evaporation—initiates a synergistic interaction between heat dissipation and water migration, which forms the basis for passive thermal regulation and freshwater harvesting. Through multiscale structural design and climate-responsive actuation, the system dynamically adjusts to environmental inputs to maintain operational stability and efficiency.

The evaporator, as shown in Fig. 2a, features a randomly entangled fibrous microstructure, as revealed by scanning electron microscopy (SEM). This porous network provides a large surface area and interconnected capillary pathways that facilitate efficient water uptake *via* capillary action. The high porosity ensures uniform distribution of water throughout the structure, thereby maximizing the effective evaporation area. Such a configuration enables rapid and sustained interfacial evaporation, continuously drawing water from the reservoir and dispersing it over the entire evaporator surface. As the water evaporates, it absorbs latent heat from the PV module, resulting in a significant reduction in the module's operating temperature. This passive evaporative cooling mechanism not only improves thermal regulation of the PV cells but also enhances overall energy conversion efficiency and extends the system's operational lifespan.

The dynamic wetting process of the evaporator surface, as shown in Fig. 2b, was captured through high-speed imaging following droplet impact. The rapid absorption of water within 0.06 seconds demonstrates the superior capillary-driven water uptake capability of the material, which is critical for sustaining continuous interfacial evaporation.[43] This result confirms the system's efficient water absorption and retention performance, both of which are essential for maintaining steady evaporation and thermal equilibrium.

The system includes a monitoring unit implemented through an Arduino-based embedded system (as shown in Fig. 2c and d) that integrates sensors (*e.g.*, a light-dependent resistor and a water level sensor) for data acquisition. Crucially, the core cooling function is achieved through the passive, capillary-driven interfacial evaporation. A small water pump is occasionally activated only when the reservoir level drops below a critical threshold, ensuring water replenishment without governing the primary cooling process.

The embedded control logic (Fig. 2e) governs system operation through a dual-threshold coordination of solar irradiance and temperature. Under low-irradiance or low-temperature conditions, the system actively inhibits water pump activation, even when the reservoir level is insufficient. This dual safeguard mechanism prevents unnecessary energy consumption and thermal regulation during non-critical periods—such as early morning, nighttime, or transient irradiance dips—when PV output is inherently limited and cooling demand is negligible. By incorporating real-time environmental feedback, the control logic dynamically transitions among operational modes (Mode 1 and Mode 2/3), maintaining an adaptive

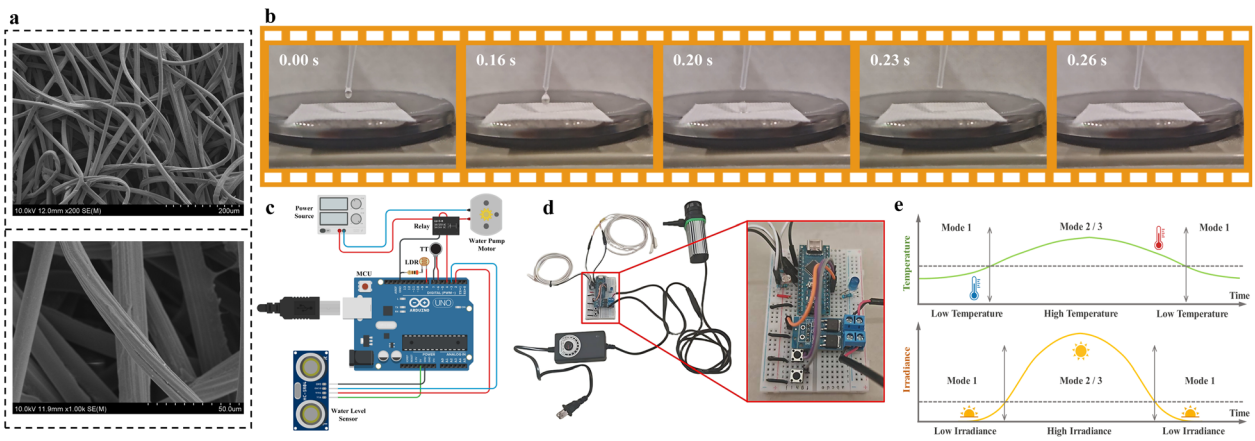

Fig. 2 Preparation and characterization of the IEWC system. (a) Scanning electron microscopy (SEM) image showing the fibrous microporous structure of the evaporator. The entangled microfibers form an interconnected porous network that facilitates efficient capillary-driven water absorption, enabling uniform moisture distribution and effective evaporative cooling. (b) Wetting performance of the evaporator, demonstrating its ability to absorb water at varying levels of saturation, contributing to the system's thermal regulation efficiency. (c) Logical wiring of the operation strategy, showing the interconnections between the core hardware components, including the Arduino microcontroller, sensors, relay, and water pump, demonstrating how they are linked *via* control signals to regulate the water pump operation. (d) Optical image of the completed control platform, showing the installed Arduino control board and its peripheral components, which enable real-time environmental monitoring and adaptive control. (e) Embedded control strategy framework, outlining the operational flow of the system, and how the sensors and actuators are integrated for seamless operation.

balance between energy harvesting, thermal management, and water resource conservation.

In summary, the IEWC system primarily leverages passive interfacial evaporation to regulate photovoltaic temperature and recover freshwater. The climate-responsive behavior is an inherent feature of this physical design, ensuring efficient operation under varying environmental conditions with minimal auxiliary energy input. This clean-energy-driven thermo–electro–hydrological coupling enables enhanced power output, prolonged device longevity, and simultaneous water generation. These features position the IEWC system as a scalable and passive solution for integrated energy and water management, particularly suitable for off-grid or arid-region applications.

2.3. Experimental setup of the IEWC system

To evaluate the performance of the IEWC system under real-world conditions, we conducted an outdoor experiment on May 30, 2025, from 10:00 AM to 5:00 PM, accounting for dynamic environmental factors such as irradiance fluctuations, wind speed, and temperature variations. The tests were conducted at North China Electric Power University (Beijing, China). The schematic of the experimental setup is shown in Fig. 3a, and a photographic image of the experimental configuration is provided in Fig. 3b.

The experimental setup was located on the roof of the university building, with two south-facing photovoltaic (PV) modules attached with a tilt angle of 36°, which was the optimum angle for the maximum exposure for solar irradiance. The main instruments that were utilized in the experiments include solar irradiance sensors, temperature probes, wind speed sensors and an acquisition system for continuous logging of the experimental conditions.

Graphical representations Fig. 3c and d illustrate the weather conditions experienced on May 30, 2025 during the experimental period. The ambient air temperature ranged from 30.6 °C to 35.8 °C during the hours of sunlight. The relative humidity (RH) ranged from 21.9% to 29.4% indicating a relatively dry condition. The maximum solar irradiance measured was 898.2 W m^{-2}, and more than 4 hours of irradiance were at or greater than 800 W m^{-2}. The wind speed was 0.89 m s^{-1} and the day had light breezes. The weather conditions were typical for a clear and sunny day in late spring, and subsequently favorable for measuring representative performance conditions

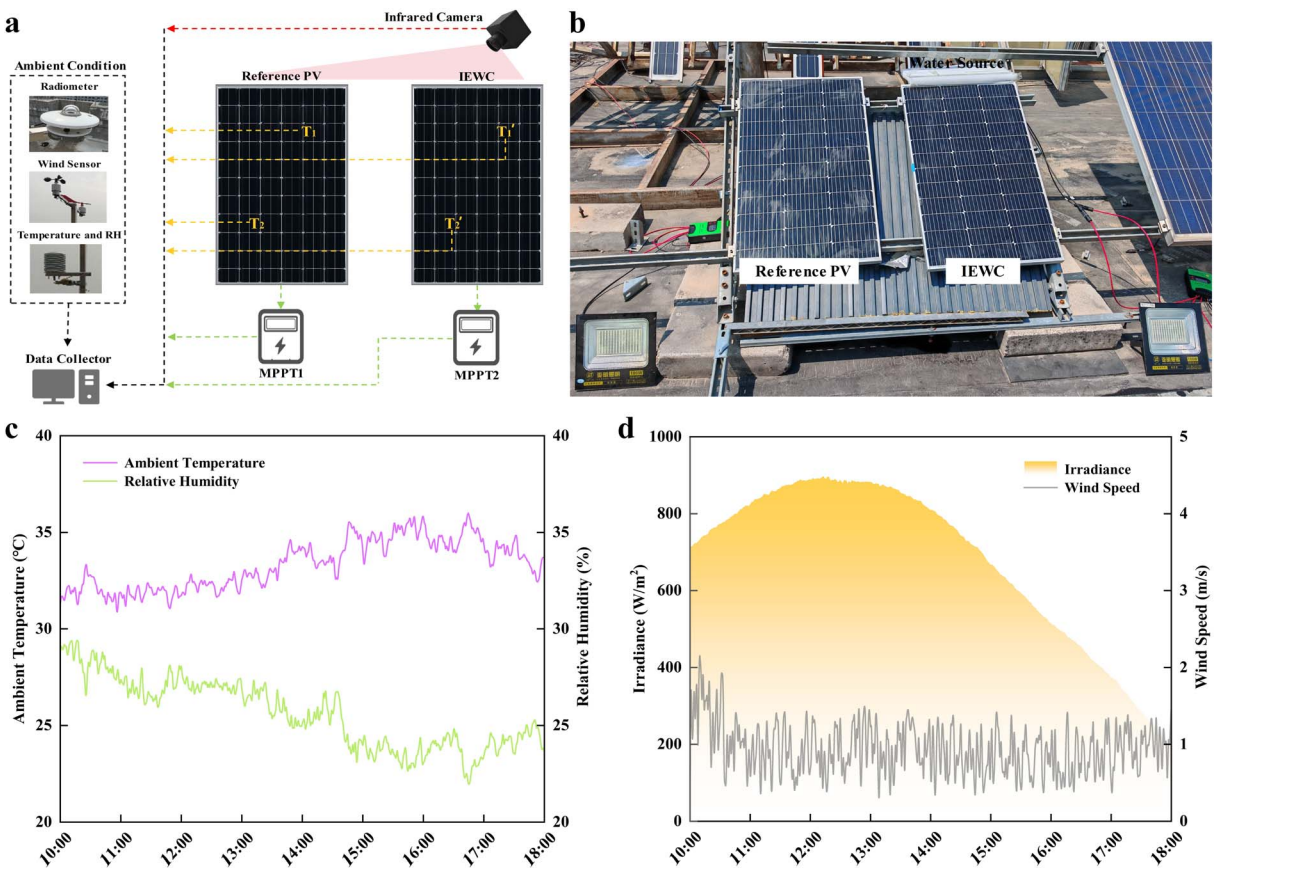

Fig. 3 Setup of field tests and meteorological conditions. (a) Schematic diagram of the experimental setup. A detailed schematic of the experimental setup used for testing the IEWC system. The diagram shows the arrangement of the PV modules, sensors, and other key components involved in the testing process. (b) Optical photo of the setup. A photo showing the actual experimental setup, including the reference PV module and the IEWC system. (c) Ambient temperature and relative humidity on May 30, 2025. (d) Irradiance and wind speed on May 30, 2025.

of the photovoltaic system. The weather data collected during the experimental period demonstrate constant solar flux, with moderate changes to temperature, which allows for testing of the IEWC system under reliable conditions.

2.4. Testing procedures and performance evaluation

The testing procedure involved systematic monitoring and measurement of key performance indicators, including cooling efficiency, power generation, and water production. Temperature measurements were recorded at multiple locations (as shown in Fig. 3a) at 1-minute intervals, allowing for real-time tracking of the cooling performance of the system. Additionally, infrared (IR) images were captured hourly to provide a detailed visual representation of temperature distribution across the module surfaces, highlighting thermal fluctuations (Fig. 4c).

The *I–V* characteristics of both the IEWC-enhanced and reference PV modules were recorded approximately every hour which allowed for varying environmental conditions to be taken into account for electrical performance. Water transfer was quantified by monitoring the mass change of the source water tank, which directly reflects the amount of water evaporated during operation. Although this measurement appears as a steady decrease in the source tank mass, it represents the vapor flux generated by interfacial evaporation and therefore corresponds to the potential freshwater yield. In the enclosed backspace of the IEWC system, most of this vapor subsequently condenses on cooler surfaces and can be recovered as distilled water. Thus, the observed mass loss from the source tank is not a permanent water consumption, but rather an indicator of evaporation-driven freshwater production.

Referring to Fig. 4a and b, temperature measurements and temperature drop values were taken for the IEWC-enhanced and standalone reference PV modules. As indicated in Fig. 4a, temperature measurements reveal that the reference module (orange line) had higher temperatures than the IEWC-enhanced module (blue line). The reference module temperatures oscillated between 34 °C and 55 °C over the testing period whereas the IEWC-enhanced module temperature was between the range of 20 °C–35 °C, reflecting a respective substantial temperature reduction throughout the day. This difference is further illustrated in Fig. 4b, where the temperature drop between the two modules is shown to range from 10 °C to 25 °C, with the largest differential occurring around midday when solar irradiance was at its peak. The maximum temperature drop reached approximately 25 °C at around 11:00 AM, emphasizing the cooling effectiveness of the IEWC system in maintaining significantly lower surface temperatures compared to the reference module. This analysis underscores the substantial cooling benefit provided by the IEWC system, which directly contributes to improved efficiency and thermal management of the PV modules under realistic operational conditions.

Fig. 4c displays the IR images showing the temperature distribution of both IEWC-enhanced and standalone PV modules taken at different times (10:30, 11:54, 13:18, 14:42, 16:06, and 17:30). These images vividly demonstrate the cooling effect of the IEWC system on the PV modules throughout the day. For instance, at 10:30, the temperature difference between the IEWC-enhanced module (33.5 °C) and the standalone module (49.4 °C) is apparent, with the IEWC module maintaining significantly lower temperatures. As the day progresses, the temperature difference diminishes, particularly at 17:30, where the temperature of the IEWC module is much lower (22.0 °C) than that of the reference module (33.9 °C). These images offer a clear visual representation of the cooling effect and the dynamic temperature variations across the modules throughout the testing period.

The I–V characteristics of both PV modules at various times during the day (10:30, 11:54, 13:18, 14:42, 16:06, and 17:30) are shown in Fig. 4d and e. The I–V curves indicate a consistent power output improvement for the IEWC-enhanced module compared to the standalone module, showcasing the influence of the cooling system on enhancing the electrical efficiency of the PV modules, particularly as temperatures increase throughout the day. The power output improvements are particularly evident during periods of high irradiance, when the temperature effects are most pronounced. Specifically, the IEWC-enhanced module shows a power output increase of 8.24% at 10:30, 8.54% at 11:54, 8.26% at 13:18, 9.15% at 14:42, 7.71% at 16:06, and 8.36% at 17:30, demonstrating consistent performance gains throughout the day.

Fig. 4f tracks the evaporated water mass through the decrease in the source tank, thereby illustrating the evaporation rate over time. This evaporated mass corresponds to the freshwater generated within the enclosed system, since condensation and recirculation occur simultaneously on cooler surfaces. As the test progresses from 10:00 to 18:00, the water mass decreases steadily, correlating with the cooling process driven by evaporation. This steady reduction in water mass further validates the cooling effect of the IEWC system, which is consistent with the improved temperature management observed in the IR images.

Together, these figures corroborate the thermal and electrical performance benefits of the IEWC system. The enhanced cooling effect leads to increased power generation, as shown by the elevated power outputs in Fig. 4d and e, alongside the visual evidence from the IR images in Fig. 4c and the consistent evaporation rates in Fig. 4f. These results highlight the IEWC system's significant improvement in both temperature regulation and electrical efficiency of the PV modules, offering a clear advantage over standalone PV modules, particularly under high-irradiance conditions.

Transitioning into a deeper analysis of the system's adaptive behavior, we examined the correlation between environmental inputs and system responses throughout the testing period. As ambient temperature and solar irradiance increased from mid-morning to early afternoon, the system passively enhanced evaporative cooling through capillary-driven water transport, sustained by intermittent pump activation solely for replenishing the upper tank water level. The increase in heat load naturally elevated the evaporation rate, reinforcing the cooling intensity without requiring active modulation of the

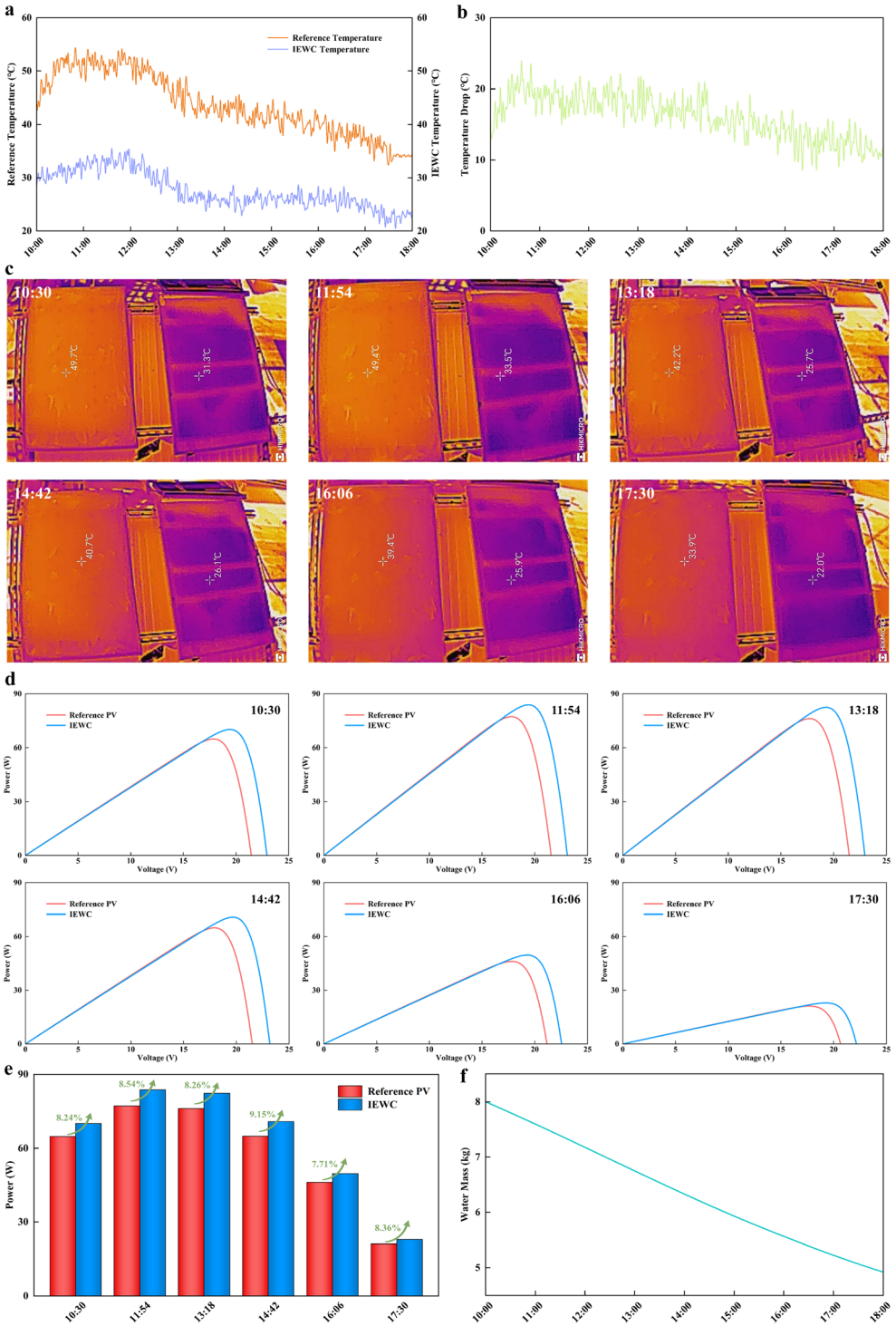

Fig. 4 Key performance indicators on May 30, 2025. (a) Temperature measurements on PV module surfaces. This plot shows the temperature measurements taken at multiple locations on the IEWC-enhanced PV module and the standalone PV module. Measurements were taken at 1-minute intervals throughout the testing period to capture dynamic cooling performance. (b) Temperature drop values. This figure shows the temperature reduction on the surfaces of the PV module with IEWC compared to the standalone module, showing how the IEWC system cooled the module. Advanced sensors also included infrared cameras to capture temperature distribution. (c) Infrared images of the temperature distribution. Infrared images were taken every 30 minutes to evaluate the temperature distribution on the surfaces of the IEWC and standalone PV modules, which displayed the temperature change during the tests. (d and e) I–V characterization of IEWC and standalone PV modules. I–V characteristics of the IEWC PV module and the standalone PV module were measured to determine the electrical performance of the system under varying photovoltaic environmental conditions. (f) Evaporation-driven water transfer. The apparent decrease in source tank mass reflects the amount of water evaporated during operation, which represents the freshwater yield of the system. In the enclosed IEWC configuration, this vapor condenses on cooler surfaces and can be recovered, enabling water–energy cogeneration. When normalized to the PV module surface area (0.525 m^2), this evaporation rate is approximately 5.72 kg m^2 per day.

evaporation interface. This environmentally responsive behavior was clearly reflected in the larger temperature differentials during peak irradiance hours (*e.g.*, 11:00–14:00), as shown in Fig. 4b, with temperature drops reaching up to 23 °C.

Traditional passive cooling systems, such as those relying solely on radiation cooling, can achieve temperature reductions (typically <10 °C), but their effectiveness diminishes at high ambient temperatures and they cannot utilize the latent heat of evaporation to further enhance cooling.[44] These systems often require large surface areas, obstruct incoming solar irradiance, and fail to recover freshwater. In contrast, the IEWC system combines passive and active mechanisms, providing significant advantages. It enhances cooling through evaporation-driven capillary transport and simultaneously collects distilled freshwater, using only ~3 kg of water per day. This dual benefit of cooling and freshwater recovery is absent in conventional active cooling systems, which require large volumes of circulating water and high energy consumption but fail to produce freshwater.[29–32]

Furthermore, as irradiance and ambient temperatures declined in the late afternoon (*e.g.*, after 16:00), the control logic of the IEWC system automatically inhibited pump operation, even as the upper tank water level decreased. This behavior, governed by dual-threshold conditions of irradiance and temperature, minimized unnecessary water replenishment and energy expenditure, ensuring efficient operation without overcooling. These transitions align with the system's dynamic shift between modes, as shown in Fig. 1e and f, showcasing real-time adaptability to environmental conditions.

Additionally, water mass data from Fig. 4f corroborate this adaptive behavior. The rate of water mass reduction was not uniform throughout the day, but peaked during high-irradiance periods, confirming that evaporation—and hence cooling strength—was adaptively modulated in response to external thermal conditions. This efficient modulation of cooling power, combined with the ability to recover freshwater, gives the IEWC system a distinct advantage over both traditional passive cooling technologies and purely active cooling systems. The synergistic coupling between passive thermal regulation and low-energy active control distinguishes the IEWC system from conventional approaches and underscores its potential for sustainable, climate-responsive operation.

2.5. Technoeconomic analysis

To support the global effort in limiting temperature rise to 1.5 °C, there is a pressing demand for energy technologies that not only offer high efficiency but also ensure long-term economic viability. The IEWC system emerges as a promising solution, attributed to its superior thermal regulation and reduced operational expenditure. This analysis benchmarks the IEWC system against representative PV cooling strategies and evaluates two key dimensions of its techno-economic potential: its comparative economic advantages and its contribution to overall PV system performance and cost-effectiveness under climate mitigation goals. Through a detailed analysis of both theoretical cost structures and implementation feasibility, this study offers insights that can inform large-scale deployment strategies. Further details on the computational framework can be found in Notes S1 and S2.

The IEWC system consistently outperforms conventional cooling technologies by exhibiting the lowest Relative Operational Level (ROL) values and the broadest ROL <1 region under varying discount rates and operation and maintenance (O&M) cost scenarios (Fig. S1–S3). When thermal energy recovery is integrated, all cooling systems maintain ROL values below 1. However, under scenarios focused solely on power generation, the ROL <1 region expands as the discount rate increases from 1% to 5%, indicating a more favorable economic outlook at higher discount rates. This effect stems from the reduced present value of future costs, making future power generation revenues more attractive relative to the initial capital investment, particularly for systems that incorporate thermal energy recovery.

As a result, PV cooling systems based solely on power generation exhibit limited economic viability at higher discount rates (*e.g.*, 5%), whereas those with thermal energy recovery show substantial improvements in performance. The economic analysis positions the IEWC system as the most cost-effective solution, underscoring its priority in PV cooling system design. By incorporating thermal energy recovery, the IEWC system enhances the competitiveness of PV cooling technologies, demonstrating the critical role of thermal energy in optimizing economic returns. Policymakers and investors should focus on advancing thermal energy recovery to maximize returns under varying economic conditions. Moreover, higher discount rates significantly amplify the benefits of integrated PV cooling systems that combine both electricity and thermal energy production, highlighting the need for supportive policies and incentives to foster adoption.

In Fig. S4, the parameters g_e and g_c—representing the annual improvement rates of the solar cell temperature coefficient and capital expenditure, respectively—are treated as a fixed ratio given their comparable influence on cost reduction. Sensitivity analyses were performed by varying one parameter (0.5%, 1%, 5%, and 10%) while keeping the other constant, revealing how cumulative cost savings respond to different rates of technological progress. The results indicate an inverse trend: faster technological advances diminish the marginal economic benefit of IEWC, whereas slower progress—more representative of current market dynamics—amplifies its relative advantage. For instance, when g_e and g_c are both set to 5%, the projected annual savings reach USD 17.48 billion, equivalent to approximately 1.6‰ of global GDP and comparable to the combined annual R&D expenditure of major solar panel manufacturers.[45]

These economic gains are accompanied by substantial environmental co-benefits, as summarized in Table S3. Under the same 5% advancement scenario, the annual reductions are estimated at 0.5‰ of global greenhouse gas emissions (≈1.82 million *t* CO_2), 0.07‰ of non-arable land area (≈5928 km^2), and 0.004‰ of global freshwater availability (≈1.23 billion *t*), equivalent to around 1.5‰ of annual global freshwater consumption.[46,47] Although these reductions are significant in their own right, IEWC's most enduring value lies in two

domains: (i) its pronounced economic returns in innovation-limited markets, where performance enhancements outweigh generic cost declines and (ii) its capacity to harness waste heat for freshwater production, delivering both water savings and new water resources. With freshwater scarcity intensifying worldwide, this dual capability—economic scalability and water resource efficiency—positions IEWC as a strategically important technology for building resilient and sustainable solar energy infrastructure.

3 Conclusions and outlook

In summary, we developed a novel Interfacial Evaporation-driven Photovoltaic Energy–Water Cogeneration (IEWC) system that integrates cooling and water recovery technologies to enhance the performance and sustainability of PV systems. By leveraging both photovoltaic and thermal effects, our system uses solar energy for electricity generation and waste heat for freshwater production through heat-driven water evaporation. The IEWC system combines a commercial PV module, a hydrophilic thin-film evaporator, and an adaptive control unit, achieving efficient thermal management and water production without external energy input. Through comprehensive techno-economic analysis, we demonstrated that the IEWC system offers the lowest Relative Operational Level (ROL) values, making it the most economically viable cooling solution across various discount rates and operational conditions. Additionally, integrating thermal energy recovery into the system boosts performance, showcasing IEWC's potential to address energy and water challenges in resource-limited areas. Our experimental results showed that the IEWC system reduced PV module temperatures by up to 23 °C, increased power output by over 8%, and produced significant amounts of freshwater under real-world conditions. With fully passive operation and consistent performance, the system provides a promising solution to global freshwater scarcity. Looking ahead, further research should focus on optimizing the system's scalability, durability, and cost-efficiency under a wider range of long-term environmental conditions, ensuring its integration with solar farms and widespread use in off-grid and arid regions. Ultimately, the IEWC system's ability to combine energy and water management in a sustainable and low-cost manner offers a promising pathway toward improving solar energy infrastructure and addressing critical global resource constraints.

Author contributions

Yang Zhao: conceptualization, methodology, software, investigation, writing – original draft. Kaitao Chen: software, investigation, validation, visualization, writing – original draft. Feng Wang: software, visualization, writing – original draft. Chao Cheng: funding acquisition, project administration, supervision, writing – review & editing. Dan Gao: data curation, funding acquisition, project administration, supervision. Heng Zhang: project administration, writing – review & editing. Jiang Yan: methodology, software, visualization. Yuting Wang: software, visualization.

Conflicts of interest

The authors declare that they have no known competing financial interests or personal relationships that could have appeared to influence the work reported in this paper.

Data availability

All relevant data that support the findings of this study are presented in the article and SI.

Supplementary information: technoeconomic analysis data and excel files; water absorption performance videos. See DOI: https://doi.org/10.1039/d5el00150a.

Acknowledgements

We gratefully acknowledge the financial support provided by the National Key R&D Program of China (2024YFF0506402 and 2021YFE0194500) and Fundamental Research Funds for the Central Universities of China (2023MS094).

References

1 Z. Mao, Y. Yao, J. Shen, *et al.*, Passive interfacial cooling-induced sustainable electricity–water cogeneration, *Nat. Water*, 2024, **2**, 93–100.
2 W. Wang, S. Aleid, Y. Shi, *et al.*, Integrated solar-driven PV cooling and seawater desalination with zero liquid discharge, *Joule*, 2021, **5**, 1873–1887.
3 F. Najafi Roudbari, H. Ehsani, S. R. Amiri, *et al.*, Advances in photovoltaic thermal systems: A comprehensive review of CPVT and PVT technologies, *Sol. Energy Mater. Sol. Cells*, 2024, **276**, 113070.
4 G. K. Singh, Solar power generation by PV (photovoltaic) technology: A review, *Energy*, 2013, **53**, 1–13.
5 C. Feng, P. Yang, H. Liu, *et al.*, Bilayer porous polymer for efficient passive building cooling, *Nano Energy*, 2021, **85**, 105971.
6 A. Boretti and L. Rosa, Reassessing the projections of the World Water Development Report, *npj Clean Water*, 2019, **2**, 15.
7 M. Herrando, K. Wang, G. Huang, *et al.*, A review of solar hybrid photovoltaic-thermal (PV-T) collectors and systems, *Prog. Energy Combust. Sci.*, 2023, **97**, 101072.
8 T. Ding and G. W. Ho, Using the sun to co-generate electricity and freshwater, *Joule*, 2021, **5**, 1639–1641.
9 G. Huang, J. Xu and C. N. Markides, High-efficiency bio-inspired hybrid multi-generation photovoltaic leaf, *Nat. Commun.*, 2023, **14**, 3344.
10 E. Radziemska, The effect of temperature on the power drop in crystalline silicon solar cells, *Renewable Energy*, 2003, **28**(1), 1–12.
11 S. Pu, J. Fu, Y. Liao, *et al.*, Promoting Energy Efficiency *via* a Self-Adaptive Evaporative Cooling Hydrogel, *Adv. Mater.*, 2020, **32**, 1907307.

12 M. Hasanuzzaman, A. B. M. A. Malek, M. M. Islam, *et al.*, Global advancement of cooling technologies for PV systems: A review, *Sol. Energy*, 2016, **137**, 25–45.
13 Q. Gong, J. Chen, Y. Zhang, *et al.*, Spectrally Engineered Coatings for Steering the Solar Photons, *Adv. Mater.*, 2025, 2502542, DOI: **10.1002/adma.202502542**.
14 X. Bao, H. Luo, T. Weng, *et al.*, Photothermal Material-Based Solar-Driven Cogeneration of Water and Electricity: An Efficient and Promising Technology, *Small*, 2025, **21**, 2411369.
15 Q. Chen, M. Burhan, F. H. Akhtar, *et al.*, A decentralized water/electricity cogeneration system integrating concentrated photovoltaic/thermal collectors and vacuum multi-effect membrane distillation, *Energy*, 2021, **230**, 120852.
16 V.-D. Dao, N. H. Vu and S. Yun, Recent advances and challenges for solar-driven water evaporation system toward applications, *Nano Energy*, 2020, **68**, 104324.
17 P. Zhang, Q. Liao, H. Yao, *et al.*, Direct solar steam generation system for clean water production, *Energy Storage Mater.*, 2019, **18**, 429–446.
18 M. Y. Wong, A. Gautam, K. Lin, *et al.*, Sustainable high-performance density—nanoporous composite wood for water evaporation-induced electricity generation, *Chem. Eng. J.*, 2025, **510**, 161729.
19 Z. Wang, Y. Wu, K. Xu, *et al.*, Hierarchical Oriented Metal–Organic Frameworks Assemblies for Water-Evaporation Induced Electricity Generation, *Adv. Funct. Mater.*, 2021, **31**, 2104732.
20 I. B. Askari and M. Ameri, Techno economic feasibility analysis of Linear Fresnel solar field as thermal source of the MED/TVC desalination system, *Desalination*, 2016, **394**, 1–17.
21 C. Li, G. Kosmadakis, D. Manolakos, *et al.*, Performance investigation of concentrating solar collectors coupled with a transcritical organic Rankine cycle for power and seawater desalination co-generation, *Desalination*, 2013, **318**, 107–117.
22 M. I. Soomro and W.-S. Kim, Performance and economic investigations of solar power tower plant integrated with direct contact membrane distillation system, *Energy Convers. Manage.*, 2018, **174**, 626–638.
23 A. Ali, R. A. Tufa, F. Macedonio, *et al.*, Membrane technology in renewable-energy-driven desalination, *Renewable Sustainable Energy Rev.*, 2018, **81**, 1–21.
24 J. Yan, W. Xiao, L. Chen, *et al.*, Superhydrophilic carbon nanofiber membrane with a hierarchically macro/meso porous structure for high performance solar steam generators, *Desalination*, 2021, **516**, 115224.
25 F. Selimefendigil, D. Okulu and H. F. Oztop, Energy and exergy performance improvement of coupled PV–TEG module by using different shaped nano-enhanced cooling channels, *Renewable Energy*, 2024, **234**, 121059.
26 M. Khayet, Solar desalination by membrane distillation: Dispersion in energy consumption analysis and water production costs (a review), *Desalination*, 2013, **308**, 89–101.
27 H. G. Teo, P. S. Lee and M. N. A. Hawlader, An active cooling system for photovoltaic modules, *Appl. Energy*, 2012, **90**, 309–315.
28 J. Siecker, K. Kusakana and B. P. Numbi, A review of solar photovoltaic systems cooling technologies, *Renewable Sustainable Energy Rev.*, 2017, **79**, 192–203.
29 S. Nižetić, D. Čoko, A. Yadav, *et al.*, Water spray cooling technique applied on a photovoltaic panel: The performance response, *Energy Convers. Manage.*, 2016, **108**, 287–296.
30 Y. Zhao, F. Wang, Z. Xu, *et al.*, Experimental and numerical investigation of spray cooling based photovoltaic/thermal system: Achieving high performance, low cost, and lightweight design, *Energy*, 2025, 135671, DOI: **10.1016/j.energy.2025.135671**.
31 R. Tripathi and G. N. Tiwari, Energy matrices, life cycle cost, carbon mitigation and credits of open-loop N concentrated photovoltaic thermal (CPVT) collector at cold climate in India: A comparative study, *Sol. Energy*, 2019, **186**, 347–359.
32 S. Abo-Elfadl, M. S. Yousef, M. F. El-Dosoky, *et al.*, Energy, exergy, and economic analysis of tubular solar air heater with porous material: An experimental study, *Appl. Therm. Eng.*, 2021, **196**, 117294.
33 S. A. Nada and D. H. El-Nagar, Possibility of using PCMs in temperature control and performance enhancements of free stand and building integrated PV modules, *Renewable Energy*, 2018, **127**, 630–641.
34 M. Rezvanpour, D. Borooghani, F. Torabi, *et al.*, Using CaCl2·6H2O as a phase change material for thermo-regulation and enhancing photovoltaic panels' conversion efficiency: Experimental study and TRNSYS validation, *Renewable Energy*, 2020, **146**, 1907–1921.
35 A. P. Raman, M. A. Anoma, L. Zhu, *et al.*, Passive radiative cooling below ambient air temperature under direct sunlight, *Nature*, 2014, **515**, 540–544.
36 Z. Wang, D. Kortge, J. Zhu, *et al.*, Lightweight, Passive Radiative Cooling to Enhance Concentrating Photovoltaics, *Joule*, 2020, **4**, 2702–2717.
37 Md. M. Hossain and M. Gu, Radiative Cooling: Principles, Progress, and Potentials, *Adv. Sci.*, 2016, **3**, 1500360.
38 P. Sakata, K. Muangnapoh, W. Rueangsawang, *et al.*, Radiative cooling film enabled by droplet-like infrared hot spots *via* low-cost and scalable spray-coating process for tropical regions, *Cell Rep. Phys. Sci.*, 2024, **5**, 101899.
39 X. Zhao, Y. Li, X. Chen, *et al.*, Radiation cooling system: Limitations, solutions, and future challenges, *Renewable Sustainable Energy Rev.*, 2025, **212**, 115428.
40 A. Tiktas, H. Gunerhan, A. Hepbasli, *et al.*, Extended exergy analysis of a novel integrated absorptional cooling system design without utilization of generator for economical and robust provision of higher cooling demands, *Energy Convers. Manage.*, 2024, **307**, 118350.
41 S. Guo, Y. Zhang, Z. Yu, *et al.*, Leaf-based energy harvesting and storage utilizing hygroscopic iron hydrogel for continuous power generation, *Nat. Commun.*, 2025, **16**, 5267.

42 S. Zhang, H. Li, S. Liu, *et al.*, Precisely manipulating polymer chain interactions for multifunctional hydrogels, *Matter*, 2025, **8**(4), 101785.
43 S. Guo, S. Patel, J. Wang, *et al.*, Self-powered green energy-harvesting and sensing interfaces based on hygroscopic gel and water-locking effects, *Sci. Adv.*, 2025, **11**, 5991.
44 B. Zhao, K. Lu, M. Hu, *et al.*, Radiative cooling of solar cells with micro-grating photonic cooler, *Renewable Energy*, 2022, **191**, 662–668.
45 World Bank. 2025; Available from: **https://data.worldbank.org/indicator/NY.GDP.MKTP.CD**.
46 Global Carbon Project. 2024; Available from: **https://globalcarbonbudget.org/gcb-2024**.
47 World Economic Forum. 2024; Available from: **https://www.weforum.org/stories/2024/10/water-demand-climate-crisis/**.